



## Individual Tracer Atoms in an Ultracold Dilute Gas

Michael Hohmann,<sup>1</sup> Farina Kindermann,<sup>1</sup> Tobias Lausch,<sup>1</sup> Daniel Mayer,<sup>1,2</sup>  
Felix Schmidt,<sup>1,2</sup> Eric Lutz,<sup>3</sup> and Artur Widera<sup>1,2\*</sup>

<sup>1</sup>*Department of Physics and Research Center OPTIMAS, University of Kaiserslautern, 67663 Kaiserslautern, Germany*

<sup>2</sup>*Graduate School Materials Science in Mainz, Gottlieb-Daimler-Strasse 47, 67663 Kaiserslautern, Germany*

<sup>3</sup>*Department of Physics, Friedrich-Alexander-Universität Erlangen-Nürnberg, 91058 Erlangen, Germany*

(Received 23 February 2017; published 30 June 2017)

We report on the experimental investigation of individual Cs atoms impinging on a dilute cloud of ultracold Rb atoms with variable density. We study the relaxation of the initial nonthermal state and detect the effect of single collisions which has so far eluded observation. We show that, after few collisions, the measured spatial distribution of the tracer atoms is correctly described by a Langevin equation with a velocity-dependent friction coefficient, over a large range of Knudsen numbers. Our results extend the simple and effective Langevin treatment to the realm of light particles in dilute gases. The experimental technique developed opens up the microscopic exploration of a novel regime of diffusion at the level of individual collisions.

DOI: 10.1103/PhysRevLett.118.263401

Diffusion is an omnipresent transport phenomenon in nature. The motion of a tagged particle in a fluid is determined by its mass  $m$  and by the density of the fluid via the Knudsen number  $K_n$  [1]. For large densities ( $K_n \ll 1$ ), the interparticle collision frequency is high and the fluid may be treated as a continuum medium. On the other hand, for low densities ( $K_n \gg 1$ ), individual collisions matter and the discrete nature of the fluid is apparent. The only closed equation applicable to all values of  $K_n$  is the Boltzmann equation for the phase-space distribution of the particles [1,2]. Solutions of this non-linear kinetic equation have been obtained in the extreme situations of vanishing and infinite Knudsen numbers, and in the Brownian limit of a heavy tracer particle,  $m/M \gg 1$ , where  $M$  is the mass of the fluid particles [1,2]. However, despite its central importance for the foundations of statistical physics and the study of, e.g., fluid flows in the upper atmosphere and aerosols dynamics [2–4], much less is known, both theoretically and experimentally, about the long-standing problem of light particles diffusing in a dilute gas at intermediate  $K_n$  [5].

An alternative and highly successful description of a tagged particle is offered by the Langevin equation [6,7]. In this stochastic approach, Newton's equation of motion for the particle is extended by friction and fluctuating forces accounting for the interaction with the surrounding gas. The Langevin equation enables simple evaluation of the macroscopic properties of the diffusing particle, without the need to compute complicated collision integrals as in the Boltzmann equation. It is valid in the Brownian limit of a heavy tracer particle, where the friction coefficient is independent of the particle velocity [8]. Recent experimental studies of Brownian motion have been reported in gases [9,10] and liquids [11,12], including studies of nonequilibrium thermodynamics [13,14]. However, the

usual Langevin equation with constant friction does not hold for light tracer particles in dilute gases [15,16].

Here, we experimentally observe the motion of individual  $^{133}\text{Cs}$  atoms impinging on a dilute cloud of ultracold  $^{87}\text{Rb}$  atoms, as shown in Fig. 1. We exploit the variable density of the cloud to automatically explore a wide range of Knudsen numbers in each experimental run, from  $K_n \approx 1$  at the center to arbitrarily large values at the edges, while  $m/M \approx 1.5$ . We initially accelerate the laser-cooled Cs atoms to a nonthermal kinetic energy of about  $43kT$  ( $T$  is the temperature of the Rb cloud and  $k$  the Boltzmann constant). We are able to investigate the nonequilibrium relaxation induced by collisions with the cloud particles, from ballistic to diffusive motion, detecting the effect of a single collision on the dynamics of the tracer atom. Discrete hard-sphere collision simulations reveal that only few collisions suffice to thermalize a Cs atom to the cloud temperature. We additionally demonstrate that the measured spatial distribution of tagged Cs atoms is well described, without any free parameters, by a generalized Langevin equation with a velocity-dependent friction coefficient [15,16]. To our knowledge, this extension of the Langevin equation has not been experimentally verified so far.

In our experiment, individual Cs tracer atoms are released from a magneto-optical trap (MOT) at  $z = -0.27$  mm and drawn toward the center of a crossed dipole trap containing an ultracold thermal Rb cloud, where all atoms are in their respective hyperfine ground state. The Rb cloud contains typically  $6 \times 10^3$  to  $3.5 \times 10^4$  atoms at a temperature of  $2 \mu\text{K}$  and with  $1/e^2$  widths of  $\sigma_r = 1.3 \mu\text{m}$  and  $\sigma_z = 39 \mu\text{m}$  in radial and axial directions [Figs. 1(a)–1(c)] [17]. After entering the cloud, a Cs atom undergoes collisions with the cold Rb atoms and thermalizes. Ultracold temperatures in the micro-Kelvin range lead to slow dynamics with thermal velocities around  $10 \text{ mm s}^{-1}$ . While at room temperature,

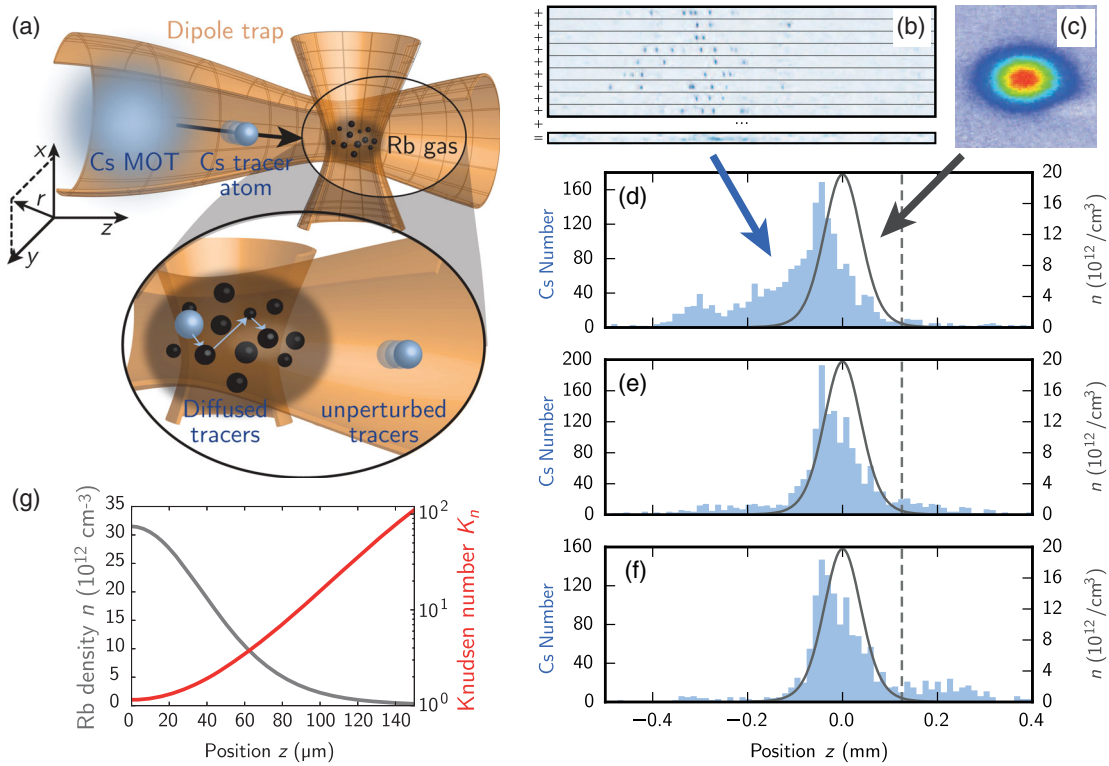


FIG. 1. (a) Sketch of the experimental setup and tracer dynamics. (b) Series of fluorescence images for identical experimental conditions, leading to a classical probability distribution of single Cs atoms. (c) Time-of-flight image of the dilute Rb cloud. (d)–(f) Measured spatial tracer distribution for a central Rb density of  $n = 2 \times 10^{13} \text{ cm}^{-3}$  for (d)  $t = 17 \text{ ms}$ , (e)  $t = 21 \text{ ms}$ , and (f)  $t = 25 \text{ ms}$ . The grey Gaussian curve indicates the Rb cloud density; right vertical scale applies. The dashed vertical line at  $z = 0.125 \text{ mm}$  separates the diffused fraction that has thermalized inside the cloud (left) from the unperturbed fraction that has passed through the cloud (right). (g) Cloud density profile and corresponding Knudsen number variation for the highest central density of  $n = 3.2 \times 10^{13} \text{ cm}^{-3}$  considered.

heavy tracer particles are bombarded at an extremely high rate (of the order of  $10^{16} \text{ Hz}$  in air [18]), ultralow temperatures, a small mass ratio of the order of unity, and low gas densities reduce this collision rate to values between  $13 \times 10^3 \text{ Hz}$  at the center and 0 at the edges of the gas cloud. Hence, the effective mean free time between two collisions is in the experimentally accessible range of  $\geq 0.1 \text{ ms}$ . For the finite-size cloud, there is a nonzero probability that a Cs atom does not collide at all and moves unperturbed through the cloud [Fig. 1(f)].

In order to observe the spatial distribution of the tagged Cs atoms, we freeze their positions after a given (interaction) time  $t$  after release from the MOT by turning on a strong 1D optical lattice in the  $z$  direction. We subsequently remove the Rb cloud from the trap and record the atomic position with fluorescence imaging [Fig. 1(b)] [19,20]. The spatial distribution for any fixed time is determined by accumulating atomic positions over about 600 realizations. The time evolution of the distribution, as it impinges on the Rb cloud, is obtained by varying the interaction time  $t$  [Figs. 1(d)–1(f)]. We use on average  $\approx 7$  Cs atoms per experimental run. Interspecies effects such as self-diffusion and self-thermalization are therefore negligible. Moreover, the thermal de Broglie wavelength is smaller than the interparticle distance

for the densities considered [21] and the dynamics of the atoms can, hence, be described classically.

Figures 2(a)–2(c) show the measured Cs spatial distributions for three increasing values of the peak Rb density  $n_{\text{max}}$  after an interaction time  $t = 25 \text{ ms}$ . For low Rb density [Fig. 2(a)], we observe a bimodal distribution with a fraction of unperturbed Cs atoms (right) that has passed through the Rb cloud (grey Gaussian curve) and a larger fraction of diffused atoms that has thermalized inside the cloud (left). The existence of the unperturbed fraction reveals the discrete nature of the dilute Rb gas. When the Rb density is increased [Figs. 2(b)–2(c)], the unperturbed fraction shrinks, as the collision probability grows with  $n_{\text{max}}$ , and the diffused fraction does not fully penetrate the cloud. With increasing density, diffusion slows down so that Cs tracer atoms need more time to reach the center of the cloud. Additionally, three-body losses become important close to the center, where the density is highest, further decreasing the number of Cs atoms. A measurement of the three-body loss rate is presented in Ref. [21]. The lifetime of a Cs atom at the peak of the spatial distribution in Fig. 2(c) is  $\tau = 3 \text{ ms}$ . Three-body losses are therefore accounted for in all simulations.

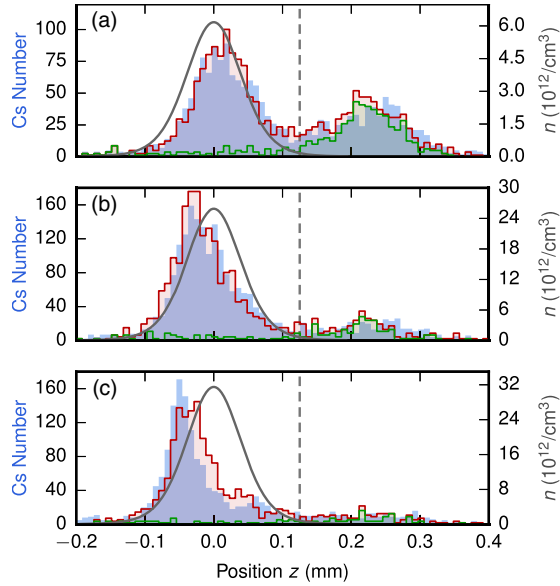


FIG. 2. Measured (blue shaded) and collision-simulated (red line) spatial distributions after an interaction time of 25 ms for Rb center densities of (a)  $n = 6 \times 10^{12} \text{cm}^{-3}$ , (b)  $n = 2.6 \times 10^{13} \text{cm}^{-3}$ , and (c)  $n = 3.2 \times 10^{13} \text{cm}^{-3}$ . The simulations are performed with 1500 atoms and normalized to the measured distribution. The agreement is excellent for both diffused (left) and unperturbed (right) fractions with an overlap larger than 90%. The unperturbed fraction is mostly composed of tracer atoms that have not suffered any collision (green, simulated).

In order to quantitatively describe the measured spatial distribution and the thermalization process, we first employ discrete hard-sphere collision simulations [21]. We numerically solve Newton's equation of motion for individual Cs tracer atoms elastically colliding with the thermal gas of Rb atoms in three dimensions. Spatial distributions as shown in Fig. 2 were obtained by projecting the atomic positions onto the  $z$  axis. A tagged Cs atom initially starts with an effective Gaussian spatial distribution at  $z = -0.27 \text{mm}$  with width  $\sigma_x = \sigma_y = 6.8 \mu\text{m}$  and  $\sigma_z = 58 \mu\text{m}$  at time  $t = 7 \text{ms}$ , and a Maxwell-Boltzmann velocity distribution with temperature  $1.4 \mu\text{K}$ . These parameters were extracted from an independent time-resolved reference measurement in the absence of the cloud. The properties of the Rb cloud were also obtained by independent measurements, so that there are no free parameters in the simulations. At each time step  $dt$ , a collision between a tracer atom and a Rb atom is described by a local collision probability,  $P_{\text{coll}} = 1 - \exp(-\Gamma dt)$ , where  $\Gamma$  is the collision rate. For nonthermal test particles with velocity  $v$ , the collision rate is given by Eq. (5.4,5) in Ref. [22],

$$\Gamma(v) = n \frac{\sigma}{\pi} \sqrt{\frac{2\pi kT}{M}} \left[ e^{-x^2} + \left( 2x + \frac{1}{x} \right) \frac{\sqrt{\pi}}{2} \text{Erf}(x) \right], \quad (1)$$

where  $\sigma$  is the scattering cross section,  $x^2 = Mv^2/(2kT)$ , and  $\text{Erf}(x)$  the error function. We analogously describe three-body losses by the probability  $P_{\text{loss}} = 1 - \exp(-dt/\tau)$ , with

the local lifetime  $\tau$  [21]. Since the density  $n$  changes spatially, the expressions above are evaluated at the current position of a tracer [30].

Results of discrete collision simulations are compared to experimental tracer distributions in Figs. 2(a)–2(c) and Ref. [21]. We obtain excellent agreement between measured (blue) and simulated (red) spatial distributions, both for the unperturbed (right) and the diffused fraction (left), with an overlap,  $(\int N_{\text{exp}} N_{\text{sim}} dz) / (\int N_{\text{exp}}^2 dz \int N_{\text{sim}}^2 dz)^{1/2}$ , between the two distributions of more than 90%. We attribute the slight discrepancies to measurement uncertainties of the independently determined parameters entering the simulations [21]. Figure 3(a) depicts the relative number of atoms in the unperturbed fraction (defined as those atoms with position  $z > 0.125 \text{mm}$ , marked by the vertical dashed line), for various values of the maximum Rb density  $n_{\text{max}}$ . The simulations show that the unperturbed fraction is mostly composed of tracer atoms that do not undergo any collision (green, simulated). The small difference between the unperturbed and noncollided fractions is due to the sharp cut at  $z = 0.125 \text{mm}$ . In addition, we find that the computed temperature difference  $\Delta T$  between the kinetic temperature of the tagged Cs atoms and the cloud temperature decays exponentially with the number of average collisions  $N_{\text{ave}}$  with a  $1/e$  decay constant of 1.3 collisions [Fig. 3(b)]. This indicates thermalization after a few collisions. We estimate, for example, a relative temperature difference of  $\Delta T/T \approx 2\%$  after  $4 \times 1.3 = 5.2$  collisions.

We next test the validity of the stochastic Langevin approach by simulating single-particle Langevin trajectories [6]. For discrete time steps  $dt$ , the Langevin equation for the velocity  $\vec{v}$  of a tagged particle takes the form [7]

$$\vec{v}(t + dt) = \vec{v}(t) + (\vec{F}_{\text{drag}} + \vec{F}_{\text{rand}} - \vec{\nabla}U) \frac{dt}{m}. \quad (2)$$

Here,  $\vec{F}_{\text{drag}} = -\gamma \vec{v}$  is a drag force with friction coefficient  $\gamma$ ,  $\vec{F}_{\text{rand}}$  a fluctuating force, and  $-\vec{\nabla}U$  the confining force including gravity. While for large, heavy test particles the friction coefficient  $\gamma$  is velocity independent, it acquires an explicit velocity dependence for small, light particles [15,16]. It is theoretically shown that [15,16,21]

$$\gamma(v) = n\sigma \frac{8}{15} \sqrt{\frac{2M}{\pi kT}} \frac{m(Mv^2/2 + 5kT)}{(m+M)} \quad (3)$$

to order  $(M/m)^{3/2}$  and for values of  $mv^2/(2kT)$  not much larger than unity. To our knowledge, the predictions of the Langevin equation with speed-dependent damping coefficient (3) have not been verified experimentally so far. We also note that owing to the detailed-balance condition, the nonlinear friction (3) implies a multiplicative, velocity-dependent fluctuating force [21,26]. We refer to Ref. [31] for a review on nonlinear Brownian motion.

Results of Langevin simulations are presented in Fig. 4 and Ref. [21]. To account for losses, tracer atoms are

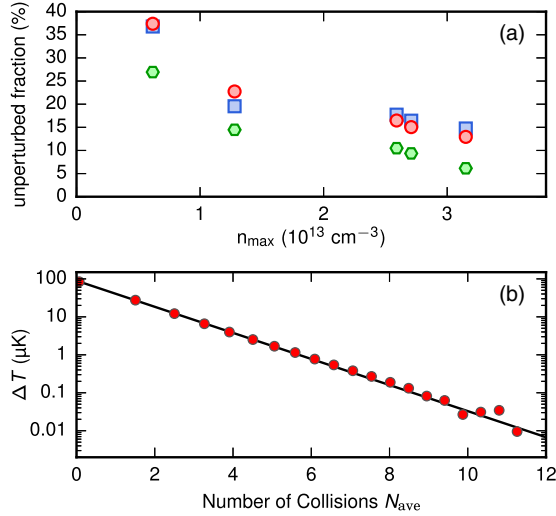


FIG. 3. (a) Measured (blue squares) and collision-simulated (red dots) relative number of atoms in the unperturbed fraction ( $z > 0.125$  mm) for various maximum Rb densities  $n_{\max}$ . Good agreement with simulated collision-free atoms (green hexagons) is observed. Error bars are smaller than the size of the symbols. (b) Simulated exponential decay of the difference  $\Delta T$  between the Cs kinetic temperature and the Rb temperature, as a function of the average number of collisions  $N_{\text{ave}}$  in a homogeneous cloud. The solid line is an exponential fit to the data with a  $1/e$  number of collisions of 1.3.

removed at each time step with probability  $P_{\text{loss}}$ . Again, cloud density  $n$ , and thus friction coefficient  $\gamma$ , were evaluated at the position of the tagged atom. We observe that the diffused fraction of Cs atoms is well described by the Langevin simulations, without free parameters, for all values of the Rb density. However, as expected, the unperturbed fraction is not captured by the Langevin approach, which assumes that all test particles experience damping and fluctuations. The overlap between the simulated and measured spatial distributions for the diffused fraction is larger than 90%. We again ascribe the small deviation to the experimental uncertainties of the reference measurements. By contrast, Langevin simulations with the usual velocity-independent friction coefficient (brown line in Fig. 4) yield overlaps as low as 60% [21]. We further note that the  $1/e$  momentum damping time  $\gamma/m \approx 250 \mu\text{s}$  for a density of  $n = 2 \times 10^{13} \text{ cm}^{-3}$ , is just a factor of 2 larger than the mean intercollision time, confirming the dominating role of individual collisions during thermalization.

The following picture emerges from our investigations. Our ability to accurately identify the effect of a single collision allows for the distinction of two different types of dynamics. Thus, Cs atoms that do not experience any collision pass ballistically through the dilute Rb cloud (unperturbed fraction). By contrast, a single collision event dissipates on average more than half of the initial non-thermal kinetic energy and suffices to trap a tagged Cs atom inside the cloud, leading to additional collisions (diffused

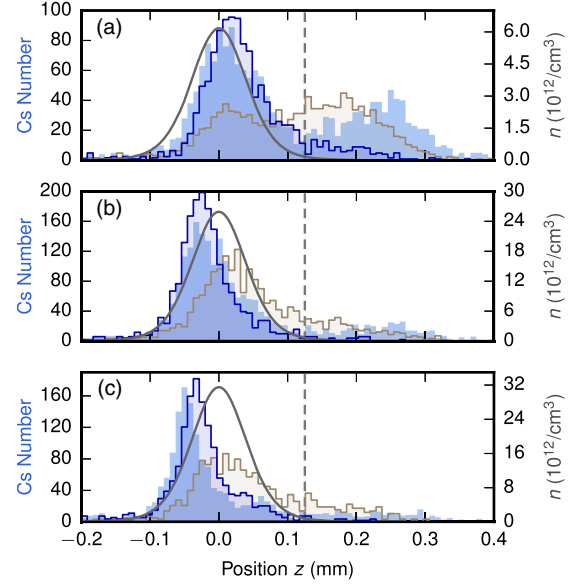


FIG. 4. Measured (blue shaded) and the Langevin-simulated spatial distribution (blue line for velocity-dependent friction, brown line for velocity-independent friction [21]) for the same data as in Fig. 2. Excellent agreement is found for the thermalized diffused fraction (left) between measured data and Langevin description based on velocity-dependent friction, with overlap larger than 90%. By contrast, the velocity-independent description yields only poor agreement with measured data with overlaps as low as 60%. In both cases, the Langevin equation (2) does not capture the unperturbed fraction (right).

fraction). After few more collisions, a tracer atom will be thermalized with the Rb cloud. Its dynamics is correctly described, over a wide range of Knudsen numbers, by a generalized Langevin equation with a velocity-dependent friction coefficient. The origin of this unfamiliar speed dependence may be understood by noting that the velocity  $v$  of a heavy Brownian particle ( $m \gg M$ ) is much smaller than that of the gas atoms. As a result, both the collision rate and the friction coefficient are independent of  $v$  in this limit. By contrast, for an atomic tracer with a mass  $m \approx M$ , both velocities are of the same order. Here, an explicit velocity dependence of the collision rate and of the friction coefficient can no longer be neglected. However, as we have shown, in both cases, a highly successful continuous Langevin description over a coarse-grained time scale larger than the mean free time between impacts is possible. The high tunability of our system further paves the way for detailed studies of diffusion in unexplored regimes. The tracer particle can be tightly controlled via, e.g., shape or dimensionality of its confining potential, including disorder, while the coupling to the bath can be adjusted via Feshbach resonances [32,33]. Finally, quantum Brownian motion could be accessed by lowering the temperature [34].

This work was partially funded by the European Union via ERC Starting Grant No. 278208 and the Collaborative

Project TherMiQ (Grant No. 618074); and by the Deutsche Forschungsgemeinschaft (DFG) via the Sonderforschungsbereich (SFB) SFB/TRR49, and the SFB/TRR185. T.L. acknowledges funding by Carl-Zeiss-Stiftung. D.M. received support from a DFG Fellowship through the Excellence Initiative by the Graduate School Materials Science in Mainz (GSC 266). F.S. acknowledges funding by the Studienstiftung des deutschen Volkes.

\*widera@physik.uni-kl.de

- [1] G. A. Bird, *Molecular Gas Dynamics and the Direct Simulation of Gas Flows* (Oxford University Press, New York, 1994).
- [2] C. Cercignani, *Rarefied Gas Dynamics: From Basic Concepts to Actual Calculations* (Cambridge University Press, Cambridge, England, 2000).
- [3] E. P. Muntz, Rarefied gas dynamics, *Annu. Rev. Fluid Mech.* **21**, 387 (1989).
- [4] F. Sharipov, *Rarefied Gas Dynamics: Fundamentals for Research and Practice* (Wiley, New York, 2016).
- [5] A. J. Masters and T. Keyes, Dependence of tagged-particle motion on size and mass, *Phys. Rev. A* **27**, 2603 (1983).
- [6] W. Coffey, Y. Kalmykov, and J. Waldron, *The Langevin Equation: With Applications in Physics, Chemistry, and Electrical Engineering* (World Scientific, Singapore, 1996).
- [7] D. Gillespie and E. Seitaridou, *Simple Brownian Diffusion: An Introduction to the Standard Theoretical Models* (Oxford University Press, New York, 2012).
- [8] P. Mazur and I. Oppenheim, Molecular theory of Brownian motion, *Physica (Utrecht)* **50**, 241 (1970).
- [9] J. Blum, S. Bruns, D. Rademacher, A. Voss, B. Willenberg, and M. Krause, Measurement of the Translational and Rotational Brownian Motion of Individual Particles in a Rarefied Gas, *Phys. Rev. Lett.* **97**, 230601 (2006).
- [10] T. Li, S. Kheifets, D. Medellin, and M. G. Raizen, Measurement of the instantaneous velocity of a Brownian particle, *Science* **328**, 1673 (2010).
- [11] R. Huang, I. Chavez, K. M. Taute, B. Lukić, S. Jeney, M. G. Raizen, and E.-L. Florin, Direct observation of the full transition from ballistic to diffusive Brownian motion in a liquid, *Nat. Phys.* **7**, 576 (2011).
- [12] S. Kheifets, A. Simha, K. Melin, T. Li, and M. G. Raizen, Observation of Brownian motion in liquids at short times: Instantaneous velocity and memory loss, *Science* **343**, 1493 (2014).
- [13] A. Béruit, A. Arakelyan, A. Petrosyan, S. Ciliberto, R. Dillenschneider, and E. Lutz, Experimental verification of Landauer's principle linking information and thermodynamics, *Nature (London)* **483**, 187 (2012).
- [14] J. Gieseler, R. Quidant, C. Dellago, and L. Novotny, Dynamic relaxation of a levitated nanoparticle from a non-equilibrium steady state, *Nat. Nanotechnol.* **9**, 358 (2014).
- [15] L. Ferrari, Particles dispersed in a dilute gas: Limits of validity of the Langevin equation, *Chem. Phys.* **336**, 27 (2007).
- [16] L. Ferrari, Particles dispersed in a dilute gas. II. From the Langevin equation to a more general kinetic approach, *Chem. Phys.* **428**, 144 (2014).
- [17] H. Metcalf and P. van der Straten, *Laser Cooling and Trapping* (Springer, New York, 2002).
- [18] R. M. Mazo, *Brownian Motion: Fluctuations, Dynamics, and Applications* (Clarendon Press, Oxford, 2002).
- [19] M. Hohmann, F. Kindermann, B. Gänger, T. Lausch, D. Mayer, F. Schmidt, and A. Widera, Neutral impurities in a Bose-Einstein condensate for simulation of the Fröhlich-polaron, *EPJ Quantum Techno.* **2**, 23 (2015).
- [20] M. Hohmann, F. Kindermann, T. Lausch, D. Mayer, F. Schmidt, and A. Widera, Single-atom thermometer for ultracold gases, *Phys. Rev. A* **93**, 043607 (2016).
- [21] See Supplementary Material at <http://link.aps.org/supplemental/10.1103/PhysRevLett.118.263401> for details, which includes Refs. [1,2,15,22,23–29].
- [22] S. Chapman and T. Cowling, *The Mathematical Theory of Non-Uniform Gases* (Cambridge University Press, Cambridge, England, 1970).
- [23] C. J. Pethick and H. Smith, *Bose-Einstein Condensation in Dilute Gases* (Cambridge University Press, Cambridge, England, 2002).
- [24] E. G. M. van Kempen, S. J. J. M. F. Kokkelmans, D. J. Heinzen, and B. J. Verhaar, Interisotope Determination of Ultracold Rubidium Interactions from Three High-Precision Experiments, *Phys. Rev. Lett.* **88**, 093201 (2002).
- [25] N. Spethmann, F. Kindermann, S. John, C. Weber, D. Meschede, and A. Widera, Dynamics of Single Neutral Impurity Atoms Immersed in an Ultracold Gas, *Phys. Rev. Lett.* **109**, 235301 (2012).
- [26] A. A. Dubkov, P. Hänggi, and I. Goychuk, Non-linear Brownian motion: The problem of obtaining the thermal Langevin equation for a non-Gaussian bath, *J. Stat. Mech. Theor. Exp.* (2009) P01034.
- [27] J. M. Sancho, M. S. Miguel, S. L. Katz, and J. D. Gunton, Analytical and numerical studies of multiplicative noise, *Phys. Rev. A* **26**, 1589 (1982).
- [28] L. Ferrari, A proper mobility formula for large, heavy particles in gases in any regime, *Chem. Phys.* **257**, 63 (2000).
- [29] M. Inguscio, S. Stringari, and C. E. Wieman, in *Bose-Einstein Condensation in Atomic Gases, Proceedings of the International School of Physics "Enrico Fermi,"* (IOS Press, Amsterdam, 1999).
- [30] We note that simulations with a homogeneous cloud with the average density fail to reproduce the observed distribution, in particular its bimodal shape. Accounting for the dilute edges of the cloud is thus essential.
- [31] Y. L. Klimontovich, Nonlinear Brownian motion, *Phys. Usp.* **37**, 737 (1994).
- [32] C. Chin, R. Grimm, P. Julienne, and E. Tiesinga, Feshbach resonances in ultracold gases, *Rev. Mod. Phys.* **82**, 1225 (2010).
- [33] T. Takekoshi, M. Debatin, R. Rameshan, F. Ferlaino, R. Grimm, H.-C. Nägerl, C. Le Sueur, J. Hutson, P. Julienne, S. Kotochigova, and E. Tiemann, Towards the production of ultracold ground-state RbCs molecules: Feshbach resonances, weakly bound states, and the coupled-channel model, *Phys. Rev. A* **85**, 032506 (2012).
- [34] U. Weiss, *Quantum Dissipative Systems* (World Scientific, Singapore, 2008).